DOI: 10.1002/ejic.201100487

Trivalent Rare Earth Complexes of the Unsymmetrical 3-(2′-Thienyl)-5-(trifluoromethyl)pyrazolate Ligand

Glen B. Deacon,*[a] Peter C. Junk,*[a] and Aron Urbatsch[a]

Keywords: Lanthanides / Rare earths / N ligands

Trivalent rare earth complexes of the unsymmetrical 3-(2′-thienyl)-5-(trifluoromethyl)pyrazolate (ttfpz) ligand, namely $[RE(ttfpz)_3(thf)_3]\cdot n$solv, where thf = tetrahydrofuran [RE = La, solv = PhMe, n = 0.5 (**1**); RE = Sm, n = 0 (**2**); RE = Tb, solv = thf, n = 1 (**3**)], $[RE(ttfpz)_3(thf)_2]$ [RE = Y (**4**), Ho (**5**), Lu (**6**), Sc (**7**)] and $[RE(ttfpz)_3(dme)_2]\cdot n$solv, where dme = 1,2-dimethoxyethane [RE = La, n = 0 (**8a**); RE = La, solv = Et_2O, n = 0.5 (**8b**); RE = Eu, solv = dme, n = 1 (**9**)], were prepared, mainly by redox transmetallation/protolysis from the free metal, $Hg(C_6F_5)_2$ and ttfpzH, and structurally characterised. In the nine-coordinate, pseudo-octahedral complexes **1** and **2**, η^2-pyrazolate and thf ligands are in a *facial* arrangement, whereas they are arranged *meridionally* in **3**. In the eight-coordinate complexes **4**–**7** the arrangement of the η^2-pyrazolate and thf ligands can be described as in between pseudo-trigonal bipyramidal and -square pyramidal. Ten-coordinate complexes **8a**, **8b** and **9** exhibit η^2-bonded pyrazolates and two chelating dme ligands as opposed to the nine-coordinate 3,5-diphenylpyrazolate (Ph_2pz) complexes $[RE(Ph_2pz)_3(dme)_2]$, which possess one unidentate and one chelating dme ligand, suggesting that the ttfpz ligand is less bulky than Ph_2pz.

Introduction

Pyrazolate ligands are attractive because of the ease of synthesis of the parent pyrazoles and their capacity for steric and electronic tuning.[1] From just three coordination modes [μ-η^1:η^1, η^2, η^1(N)] in the late 1990s,[2] over twenty are now known, underlining their versatility and flexibility. The thermal stability of the complexes has led to their application in metal organic chemical vapour deposition,[3,4] particularly for lanthanoid complexes[5–7] (other ligands are preferred for atomic layer deposition, see Ref.[8]), and has enabled the synthesis of homoleptic rare earth and alkaline earth complexes from the elements and pyrazoles at elevated temperatures.[9] As the structural chemistry of alkaline earth pyrazolates is dominated by symmetrical 3,5-disubstituted ligands, R_2pz (pz = pyrazolate; R = Me, *t*Bu, *i*Pr, Ph, H)[1] (for exceptions see Refs.[10,11]), we introduced the unsymmetrical 3-(2′-thienyl)-5-(trifluoromethyl)pyrazolate (ttfpz) ligand[12] in complexes with Ca, Sr, Ba and Yb^{II}.[13] Of particular interest was whether the differences between the two substituents would affect the dominant η^2-binding exhibited by these metals in $[M(R_2pz)_2(solv)_n]$ complexes or whether more subtle differences would be observed. Not only are the steric effects of CF_3 (spherical) and thienyl (planar) groups different, but the N–M interaction adjacent to the CF_3 group might be weakened by its electron-withdrawing nature leading to asymmetry in η^2-coordination. Other possibilities include N,S chelation rather than η^2-*N*,*N*′-binding (see S-thienyl–rare earth ligation Refs.[14,15]), weak C–F–M interactions[16–18] or even C–F activation.[19] In the event, the domination of η^2-binding for these elements[1,2] was not subverted, and asymmetric chelation occured. Furthermore, interesting differences to the corresponding Ph_2pz complexes were observed. For example, in the *trans*-$[Ba(pz)_2(thf)_4]$ derivatives, the pyrazolate rings are coplanar for ttfpz,[13] but perpendicular for Ph_2pz;[14] $[M(ttfpz)_2(dme)_2]$ (M = Ca, Sr) complexes[13] have *transoid* stereochemistry, whereas the corresponding Ph_2pz complexes are *cisoid*.[14] Although Ca^{2+} and Yb^{2+} have similar ionic radii,[15] $[Yb(ttfpz)_2(dme)_2]$ is *cisoid*,[13] and can be prepared by redox transmetallation/protolysis from Yb metal, $Hg(C_6F_5)_2$ and ttfpzH,[13] whereas the analogous synthesis with Ph_2pzH[10] led to gross decomposition. We have now examined rare earth ttfpz derivatives in the trivalent state. Addition of a third ttpfz ligand and the smaller size of most RE^{3+} ions should increase the effect of the asymmetric ligand and provide a better indication of its steric effect. Accordingly, the synthesis and characterisation of $[RE(ttfpz)_3(thf)_3]$, $[RE(ttfpz)_3(thf)_2]$ and $[RE(ttfpz)_3(dme)_2]$ are reported with the structures showing marked differences from those of related complexes with symmetric R_2pz ligands.

Results and Discussion

Syntheses and Characterisations

Complex synthesis was carried out according to reaction (1) (Scheme 1) from bis(pentafluorophenyl)mercury, 3-

[a] School of Chemistry, Box 23, Monash University, Clayton, Victoria 3800, Australia
E-mail: peter.junk@monash.edu
glen.deacon@monash.edu

(2′-thienyl)-5-(trifluoromethyl)pyrazole (ttfpzH) and an excess of RE metal in thf or dme under a nitrogen atmosphere. The air- and moisture-sensitive trivalent complexes [RE(ttfpz)$_3$(thf)$_3$]·*n*solv [RE = La, solv = PhMe, *n* = 0.5 (**1**); RE = Sm, *n* = 0 (**2**)], [RE(ttfpz)$_3$(thf)$_2$] [RE = Y (**4**), Ho (**5**), Lu (**6**), Sc (**7**)] and [RE(ttfpz)$_3$(dme)$_2$]·*n*solv [RE = La, *n* = 0 (**8a**); RE = La, solv = Et$_2$O, *n* = 0.5 (**8b**); RE = Eu, solv = dme, *n* = 1 (**9**)] were isolated in moderate to good yields (46–79%).

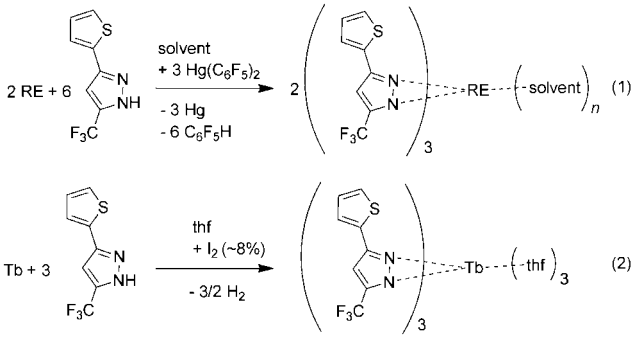

Scheme 1. Synthesis of **1**–**9**.

In addition, [Tb(ttfpz)$_3$(thf)$_3$]·thf (**3**) was isolated in low yield following the reaction of I$_2$-activated Tb with ttfpzH in thf [reaction (2), Scheme 1]. This reaction was up to five times slower than the other complexation reactions with the organomercurial Hg(C$_6$F$_5$)$_2$. Blank reactions involving Y, Tb and Eu metals and ttfpzH in thf only gave crystals of ttfpzH. We earlier reported a good yield of [La(Ph$_2$pz)$_3$(dme)$_2$]·dme from the redox transmetallation reaction between I$_2$-activated La metal and SnMe$_2$(Ph$_2$pz)$_2$[16] and are currently completing a study of the formation of rare earth 2,6-diisopropylphenolates by reaction of I$_2$-activated rare earth metals with 2,6-diisopropylphenol.[17]

The compounds were characterised by single-crystal X-ray diffractometry, melting point and elemental analyses and IR and ^{1}H NMR spectroscopy. No N–H stretching absorptions at 3150–3300 cm^{-1} were observed in the IR spectra and no N–H resonances were observed in the ^{1}H NMR spectra, both observations indicating complete deprotonation of the pyrazole. The composition of the crystals, as determined by single-crystal X-ray diffraction, was also confirmed for the bulk samples by matching solvent to ligand ratios in the ^{1}H NMR spectra. However, in the fractional toluene solvated complex **1**, the methyl group proton integration showed that some toluene was lost upon preparation of the sample for NMR measurements (the aromatic protons are masked by the solvent signal). For complexes **3**, **5** and **9**, the strongly paramagnetic metals (Eu, Tb and Ho) prevented characterisation by NMR spectroscopy. Several of the complexes were crystallised from diethyl ether without displacement of the coordinated thf or dme molecules and without incorporation of lattice solvent except for **8b** (a hemiether solvate). Elemental or metal analyses confirmed the proposed stoichiometries in all cases, except for **3** where the microanalysis fitted for the loss of lattice solvent and **9** where the metal analysis indicated the loss of two molecules of dme from the structural formula derived from X-ray crystallography. ^{19}F NMR measurements revealed one resonance at around –59 to –60 ppm for the freely rotating CF$_3$ group for all compounds. The effect of paramagnetism on **2** was negligible.

Structural Studies

[RE(ttfpz)$_3$(thf)$_3$]·nsolv Complexes

Complexes **1**, **2** and **3** are monomeric, nine-coordinate (Figure 1) pyrazolatolanthanoid(III) species with three η^2-bonded ttfpz ligands and three coordinated thf molecules. All three complexes crystallise in the triclinic space group $P\bar{1}$ (Table 1). The pseudo-octahedral **1** and **2** are isostructural (Figure 1, top), **1** being solvated by half a molecule of toluene per complex molecule. Complex **3** (Figure 1, bottom) possesses the same composition and is solvated by one disordered thf molecule.

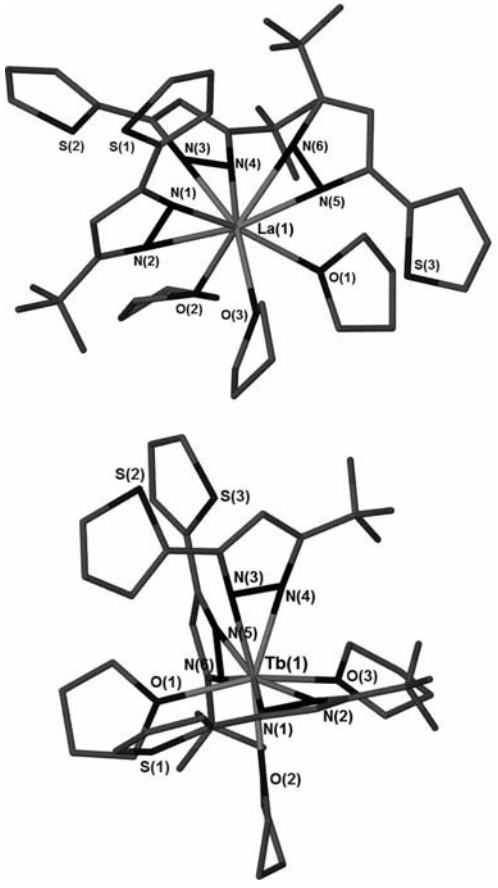

Figure 1. Crystal structure of **1** (top, also representative of **2**) and **3** (bottom). Disordered components of thienyl groups, CF$_3$ groups, thf ligands, all hydrogen atoms and the lattice solvent molecules are omitted for clarity.

In **1** and **2**, the ligands are arranged in a *facial* arrangement, one hemisphere of the coordination sphere contains only ttfpz ligands and the other only thf molecules. This is exemplified by observation of *transoid* cen(NN)–RE–O angles [cen(NN) = midpoint of N–N bond]. The Tb^{3+} ion

Table 1. Crystallographic data for complexes **1**–**3**.

	1	**2**	**3**
Chemical formula	$2(C_{36}H_{36}F_9LaN_6O_3S_3)\cdot C_7H_8$	$C_{36}H_{36}F_9N_6O_3S_3Sm$	$C_{36}H_{36}F_9N_6O_3S_3Tb\cdot C_4H_8O$
Formula mass	2105.73	1018.24	1098.91
Crystal system	triclinic	triclinic	triclinic
Space group	$P\bar{1}$	$P\bar{1}$	$P\bar{1}$
a /Å	9.8720(2)	9.7471(3)	11.4120(3)
b /Å	10.3604(2)	10.2848(4)	12.6641(4)
c /Å	21.8234(4)	20.7866(7)	17.4829(5)
α /°	86.143(1)	103.431(2)	74.019(1)
β /°	78.014(1)	93.041(2)	81.549(1)
γ /°	83.988(1)	96.552(2)	70.077(1)
Unit cell volume/Å^3	2169.0(7)	2006.73(12)	2279.70(11)
Number of formula units per unit cell, Z	1	2	2
Number of reflections measured	36516	23079	31843
Number of independent reflections	9848	8606	10212
R_{int}	0.0216	0.0416	0.0304
Final R_1 values [$I > 2\sigma(I)$]	0.0296	0.0801	0.0501
Final $wR(F^2)$ values [$I > 2\sigma(I)$]	0.0688	0.1673	0.1248
Final R_1 values (all data)	0.0350	0.0873	0.0527
Final $wR(F^2)$ values (all data)	0.0714	0.1710	0.1260
Goodness-of-fit on F^2	1.032	1.328	1.255

Table 2. Selected bond lengths [Å] and angles [°] for **1**–**3**.

	1	**2**	**3**
Bond lengths			
Ln(1)–N(1)	2.513(2)	2.414(7)	2.412(4)
Ln(1)–N(2)	2.576(2)	2.491(7)	2.431(5)
Ln(1)–N(3)	2.511(2)	2.409(7)	2.393(5)
Ln(1)–N(4)	2.575(2)	2.518(7)	2.401(5)
Ln(1)–N(5)	2.563(2)	2.502(7)	2.397(4)
Ln(1)–N(6)	2.503(2)	2.419(7)	2.495(4)
Ln(1)–O(1)	2.5625(18)	2.467(6)	2.407(3)
Ln(1)–O(2)	2.5741(18)	2.496(6)	2.440(4)
Ln(1)–O(3)	2.5722(18)	2.492(5)	2.405(4)
Bond angles			
O(1)–Ln–O(2)	78.19(6)	77.9(2)	82.54(13)
O(2)–Ln–O(3)	88.18(6)	88.20(19)	79.30(15)
O(1)–Ln–O(3)	74.51(6)	75.43(19)	148.88(14)
Centroid angles[a]			
cen{N(1)N(2)}–Ln–O(1)	154.7	155.31	101.1
cen{N(3)N(4)}–Ln–O(2)	166.2	165.8	162.2
cen{N(1)N(2)}–Ln–O(3)	156.1	156.6	79.8
cen{N(1)N(2)}–Ln–cen{N(3)N(4)}	103.3	103.7	83.3
cen{N(3)N(4)}–Ln–cen{N(5)N6})	96.5	96.7	99.7
cen{N(1)N(2)}–Ln–cen{N(5)N(6)}	105.2	105.2	177.0

[a] Centroid positions not refined.

(smaller than La^{3+} and Sm^{3+})[15] requires the ligands to realign resulting into a *meridional* arrangement in **3**. This may be seen from the O–Ln–O and cen(NN)–RE–cen(NN) angles, as well as from angles between the thf and ttfpz ligands. A *trans*-cen(NN)–RE–cen(NN) and a *transoid* O–Ln–O angle are observed only in **3** (Table 2). Related Ph_2pz complexes $[Ln(Ph_2pz)_3(thf)_3]$ (Ln = Nd, Sm)[18,19] display a *meridional* arrangement of the ligands, in contrast to **1** and **2** (Scheme 2).

The effect of the CF_3 and thienyl substituents on the adjacent RE–N bond lengths is not clear. In **1** and **2**, all pyrazolate ligands are unsymmetrically chelating. Two ligands

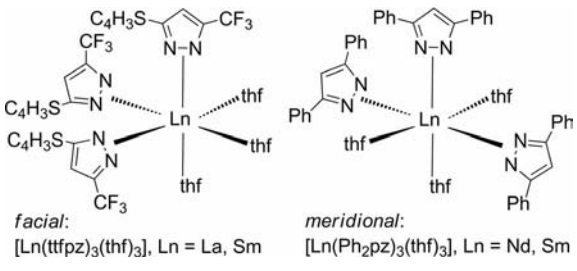

Scheme 2. Comparison of $[Ln(ttfpz)_3(thf)_3]$ and $[Ln(Ph_2pz)_3(thf)_3]$.

[N(1,2), N(3,4)] have longer bonds from the N atom adjacent to the CF_3 group, consistent with its electron-withdrawing properties, but ligand N(5,6) shows the reverse behaviour. By contrast, **3** has two symmetrically bound ligands [N(1,2), N(3,4)] and ligand N(5,6) has a longer Tb–N bond to the nitrogen atom adjacent to the CF_3 group. Accordingly, overall packing considerations must override steric/electronic effects of the disparate substituents. With $[M(ttfpz)_2(thf)_4]$[13] (M = Yb, Ca, Sr, Ba) complexes, M–N adjacent to CF_3 is shorter, whereas in $[M(ttfpz)_2(dme)_2]$[13] (M = Yb, Ca, Sr) and $[Ba(ttfpz)_2(dme)_3]$,[13] either M–N adjacent to CF_3 is longer (Yb, Ba) or the coordination is symmetrical. Comparing *fac*-**2** with *mer*-$[Sm(Ph_2pz)_3(thf)_3]\cdot 3thf$,[19] the average Sm–N bond lengths are comparable (2.46 Å to 2.44 Å, respectively) despite the stereochemical difference, but the range of bond lengths is somewhat larger in **2**, presumably a result of the unsymmetrical substitution.

The average Ln–N bond lengths, 2.54 Å in **1**, 2.46 Å in **2** and 2.42 Å in **3**, follow the lanthanoid contraction well, the differences (0.08 and 0.04 Å, respectively) being close to the differences in ionic radii between nine-coordinate La/Sm and Sm/Tb (Δ = 0.084 and 0.037 Å, respectively).[15] Increased steric crowding does not lead to relative bond lengthening.

Average Ln–O distances for the thf ligands follow the decrease in ionic radii well between complexes **1** and **2** (Δ = 0.08 Å), but they decrease more than expected between complexes **2** and **3** (Δ = 0.07 Å). These observations may be explained by the *trans*-influence of the pyrazolate ligands (see, for example, ref.[18,20–23]) on the Ln–O bond lengths in *fac* complexes **1** and **2**. In these, all thf donors are *transoid* to a pyrazolate ligand, which leads to elongation of the Ln–O bonds. In *meridional* **3**, only thf molecule O(2) is *transoid* with a cen{N(3)N(4)}–Tb(1)–O(2) angle of 162.2° (Table 2), leading to elongation of the Tb(1)–O(2) bond compared with the Tb(1)–O(1/3) bonds (Table 2). On the other hand, <Sm–O> of **2** (2.48 Å) is less than that (2.54 Å) of $[Sm(Ph_2pz)_3(thf)_3]\cdot 3thf$,[19] perhaps indicative of the greater steric bulk of Ph_2pz than ttfpz. The change in stereochemistry from *facial* to *meridional* for complexes **1**–**3** contrasts with the six-coordinate $[RE(dbp)_3(thf)_3]$[24] (RE = La, Pr, Nd, Gd, Er; dbp = 2,4-di-*tert*-butylphenolate) complexes, where a *meridional* arrangement is observed for RE = La–Gd, the larger lanthanoid metals, but a *facial* arrangement for Er.

A consequence of the increased steric crowding from **1**–**3** is a decrease in disorder of the thienyl groups. Complexes **1** and **2** show disorder of the thienyl groups (and small parts of the thf molecules), whereas **3** does not show disorder, suggesting the ligands in **3** are "locked" into one position. More evidence of crowding in **3** is that the thienyl groups are not coplanar with the pyrazolate rings (twisted by about 17.4–23.8°), whereas they are coplanar in **1** and **2**.

[RE(ttfpz)$_3$(thf)$_2$] Complexes

With lanthanoid metals heavier than Tb and the rare earth metals Sc and Y, the isomorphous $[RE(ttfpz)_3(thf)_2]$ complexes **4**–**7** (Figure 2) crystallise in the orthorhombic space group *Pbca* without the inclusion of lattice

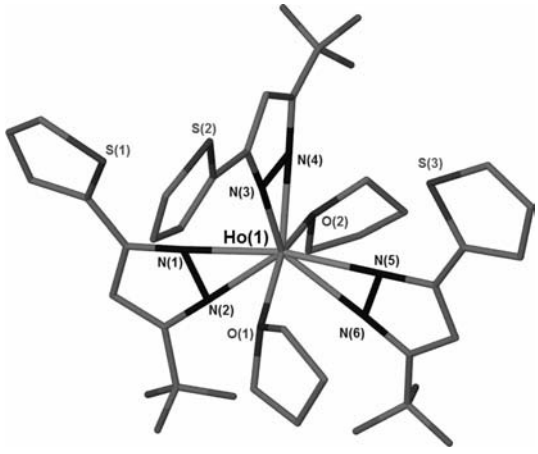

Figure 2. Crystal structure of **5**, representative of **4**–**7**. All hydrogen atoms are omitted for clarity.

Table 3. Crystallographic data for **4**–**7**.

	4	**5**	**6**	**7**
Chemical formula	$C_{32}H_{28}F_9N_6O_2S_3Y$	$C_{32}H_{28}F_9HoN_6O_2S_3$	$C_{32}H_{28}F_9LuN_6O_2S_3$	$C_{32}H_{28}F_9N_6O_2S_3Sc$
Formula mass	884.69	960.71	970.75	840.74
Crystal system	orthorhombic	orthorhombic	orthorhombic	orthorhombic
Space group	*Pbca*	*Pbca*	*Pbca*	*Pbca*
a/Å	17.2161(14)	16.6232(6)	16.6859(11)	16.9964(6)
b/Å	20.7336(15)	20.6993(7)	20.6182(14)	20.1681(7)
c/Å	21.1558(17)	21.1635(7)	21.1615(14)	21.0051(7)
Unit cell volume/Å^3	7551.6(10)	7282.1(4)	7280.3(8)	7200.2(4)
Number of formula units per unit cell, *Z*	8	8	8	8
Number of reflections measured	117800	171254	49687	81892
Number of independent reflections	8677	8348	8352	8165
R_{int}	0.1015	0.0761	0.0954	0.0983
Final R_1 values [$I > 2\sigma(I)$]	0.0650	0.0950	0.0730	0.0762
Final $wR(F^2)$ values [$I > 2\sigma(I)$]	0.1824	0.1642	0.1356	0.1443
Final R_1 values (all data)	0.1218	0.1066	0.1079	0.1147
Final $wR(F^2)$ values (all data)	0.2198	0.1679	0.1462	0.1613
Goodness-of-fit on F^2	1.056	1.311	1.354	1.062

Table 4. Selected bond lengths [Å] and angles [°] for **4**–**7**.

	4	**5**	**6**	**7**
[RE(ttfpz)$_3$(thf)$_2$]	Y	Ho	Lu	Sc
Bond lengths				
RE(1)–N(1)	2.342(4)	2.345(7)	2.301(7)	2.193(3)
RE(1)–N(2)	2.356(4)	2.354(8)	2.314(8)	2.209(3)
RE(1)–N(3)	2.313(4)	2.320(8)	2.280(7)	2.182(3)
RE(1)–N(4)	2.348(4)	2.358(7)	2.329(7)	2.225(3)
RE(1)–N(5)	2.346(4)	2.336(8)	2.301(8)	2.182(3)
RE(1)–N(6)	2.394(5)	2.377(8)	2.353(7)	2.281(3)
RE(1)–O(1)	2.343(4)	2.366(7)	2.298(7)	2.223(3)
RE(1)–O(2)	2.338(4)	2.338(7)	2.303(7)	2.200(3)
Bond angle				
O(1)–RE–O(2)	152.94(14)	155.0(2)	154.5(2)	153.11(10)
Centroid angles[a]				
cen{N(1)N(2)}–RE–O(1)	86.1	87.3	87.3	86.7
cen{N(1)N(2)}–RE–O(2)	86.8	86.8	87.7	88.0
cen{N(3)N(4)}–RE–O(1)	103.1	101.7	101.7	103.0
cen{N(3)N(4)}–RE–O(2)	103.6	103.6	103.4	103.6
cen{N(5)N(6)}–RE–O(1)	81.0	81.1	81.1	81.3
cen{N(5)N(6)}–RE–O(2)	86.6	86.1	85.2	84.7
cen{N(1)N(2)}–RE–cen{N(3)N(4)}	111.5	112.5	111.5	110.9
cen{N(3)N(4)}–RE–cen{N(5)N(6)}	111.2	112.6	112.7	112.4
cen{N(1)N(2)}–RE–cen{N(5)N(6)}	137.2	134.8	135.7	136.6

[a] Centroid positions not refined.

solvent (Table 3). All are eight-coordinate species with exclusively η^2-bonded ttfpz ligands and two thf ligands, in contrast to **1**–**3**. Ligands N(1,2) and N(5,6) are on opposite sides of the metal, with their ring planes (defined by the pyrazolate rings) close to coplanar [in **7** the angle is 13.76(13)°]. Both the CF_3 as well as the 2-thienyl groups of ligands N(1,2) and N(5,6) face each other and the 2-thienyl groups are separated by ttfpz ligand N(3,4). Ligand N(3,4) is mutually perpendicular to ligands N(1,2) and N(5,6) [angles between their mean planes are N(1,2)/N(3,4) 83.30(13)° and N(5,6)/N(3,4) 83.40(12)°]. The thf ligands are close to normal to ligands N(1,2) and N(5,6) (Figure 2) as shown by the cen(NN)–RE–O angles (Table 4).

The coordination geometry around the metals can best be described as an intermediate between pseudo-square pyramidal (sp) and -trigonal bipyramidal (tbp). For the latter case (tbp), thf oxygen atoms O(1) and O(2) are apical and the centroids of the pyrazolate ligands are in the equatorial position. For the former case (sp), centroid [N(3)N(4)] is considered apical and the *transoid* centroids [N(1)N(2)] and [N(5)N(6)] and the O(1), O(2) donors are in the square plane. A similar arrangement has been reported in the related complexes [Ln(*t*Bu$_2$pz)$_3$(thf)$_2$] (Ln = Nd,[25,26] Er;[26] *t*Bu$_2$pz = 3,5-di-*tert*-butylpyrazolate), [Yb(Ph$_2$pz)$_3$(thf)$_2$]·2C$_6$D$_6$[16] and [RE(Ph$_2$pz)$_3$(Ph$_2$pzH)$_2$][27] (RE = La, Nd, Gd, Er, Yb). The O–Ln–O angles of the *t*Bu$_2$pz complexes [145.2(6)° (Ln = Nd), 140.1(4)° (Ln = Er)] are smaller than those of complexes **4**–**7** (Table 4), whereas the corresponding angle in [Yb(Ph$_2$pz)$_3$(thf)$_2$]·2C$_6$D$_6$,[16] [153.45(7)°] and the related N–RE–N angles of [RE(Ph$_2$pz)$_3$(Ph$_2$pzH)$_2$][27] are similar. There is also correspondence between the cen(NN)–RE–cen(NN) angles of **4**–**7** (Table 4) with [Ln(*t*Bu$_2$pz)$_3$(thf)$_2$] (two angles of 110° and one of 140°)[25,26] and [Yb(Ph$_2$pz)$_3$(thf)$_2$]·2C$_6$D$_6$ (two of 111° and one of 138°).[16]

As observed in the preceding series, the η^2-bonded ttfpz ligands are mainly unsymmetrically coordinated. Longer RE–N bonds are observed on the trifluoromethyl group side than those adjacent to the 2-thienyl group (Table 4), consistent with the electronic effects of the substituents. The average difference rises from ca. 0.03 Å for **4** to 0.05 Å for **7**, mainly due to the large difference of 0.099 Å between Sc(1)–N(5) and Sc(1)–N(6) (Table 4). Since the isomorphous complexes **4**–**6** display similar N(6)–RE(1)–N(1–5) angles to **7**, thereby excluding differential *trans*-influence from ligand N(1,2), this asymmetry may be explained by the increase in steric crowding as scandium possesses the smallest ionic radius in the series.[15] In **1**–**3**, a similar elongation of RE–N(6) is observed in **3**, the most crowded complex of the series.

The <RE–N> bond lengths follow the trend in ionic radii of RE^{3+}. Thus, <RE–N> bond lengths in **4** and **5** (2.35 Å) are almost indistinguishable, as are the eight-coordinate ionic radii of Y^{3+} and Ho^{3+},[15] and from **6** to **7** the contraction of the <RE–N> bond lengths matches the difference in ionic radii.

In addition, <RE–N> of **6** is similar to that of [Yb(Ph$_2$pz)$_3$(thf)$_2$]·2C$_6$D$_6$,[16] Lu^{3+} and Yb^{3+} having similar ionic radii.[15] The RE–O bond lengths of the two thf donors are similar, and those of **6** are somewhat shorter than those of [Yb(Ph$_2$pz)$_3$(thf)$_2$]·2C$_6$D$_6$,[16] suggesting that Ph$_2$pz is bulkier than ttfpz.

Comparison of the chemistry of **1**–**7** with the corresponding *t*Bu$_2$pz and Ph$_2$pz complexes provides evidence of

the relative steric demand of the ligands. Thus, nine-coordinate **1**–**3** compare with eight-coordinate $[Nd(tBu_2pz)_3(thf)_2]$[25] ($La^{3+} > Nd^{3+} > Sm^{3+} > Tb^{3+}$ in ionic radii),[15] and probably $[La(tBu_2pz)_3(thf)_2]$ based on composition,[26] indicating that tBu_2pz is bulkier than ttfpz. With **1**–**7**, a change from nine-coordination (*fac*-**1**, *fac*-**2**, *mer*-**3**) to eight-coordination occurs after Tb. In the three crystallographically characterised Ph_2pz complexes $[Ln(Ph_2pz)_3(thf)_n]$ (Ln = Nd,[18] Sm,[19] n = 3; Ln = Yb,[16] n = 2), the first two are nine-coordinate and the last eight-coordinate. Although the point of change is not known, the composition of the Gd complex corresponds to $[Gd(Ph_2pz)_3(thf)_2]$[28a] suggesting that the nine → eight-coordinate change occurs with a larger RE than for **1**–**7**, consistent with greater steric bulk for Ph_2pz than ttfpz. Both the symmetrically substituted tBu_2pz and Ph_2pz complexes show unsymmetrical pyrazolate coordination of a magnitude similar to those of complexes **1**–**7** and of the divalent complexes $[M(ttfpz)_2(thf)_4]$[13] (M = Yb, Ca, Sr, Ba) and $[M(ttfpz)_2(dme)_n]$[13] (M = Yb, Ca, Sr, n = 2; M = Ba, n = 3), suggesting that the different steric and electronic effects of the CF_3 and thienyl substituents may offset each other.

[RE(ttfpz)$_3$(dme)$_2$]·nsolv Complexes

Obtained from reactions in dme, **8a**, **8b** and **9** have ten-coordinate lanthanoid ions, which are surrounded by three η^2-bonded ttfpz ligands and two chelating dme donors (Figure 3). No previous $[RE(pz)_3(dme)_2]$ complexes are ten-coordinate. Complex **8a** crystallises in the monoclinic space group *Cc* with no lattice solvent, whereas **8b** and **9** crystallise in the monoclinic space group $P2_1/n$, (two discrete complex molecules are found in the asymmetric unit) and are isomorphous with each other (Table 5) even though they are differently solvated, with 0.5 Et_2O in **8b** and 1.0 dme in **9**.

The <RE–N> bond length decreases from 2.57 Å in **8a** and 2.56 Å in **8b** to 2.45 Å in **9**. This difference is as expected from ionic radii differences.[15] Longer RE–N bonds adjacent to the CF_3 groups than to the 2-thienyl groups are observed (Table 6), and the asymmetry in the bond lengths of **8a** and **8b** is larger than in **4**–**7**. For example, in **8a** the La–N bond on the CF_3 side is 0.09 Å longer than that on the 2-thienyl side (cf. 0.03 Å–0.05 Å for **4**–**7**). In **9** the asymmetry (0.055 Å) is also substantial. Chelation of the dme ligands in **8a** and **8b** is very unsymmetrical (0.082–0.106 Å) and far more than in **9** (0.044 and 0.011 Å). The difference in <RE–O> between **8a**/**8b** and **9** (0.07 Å) is less than expected from ionic radii differences, and consistent with increased steric stress in **9**.

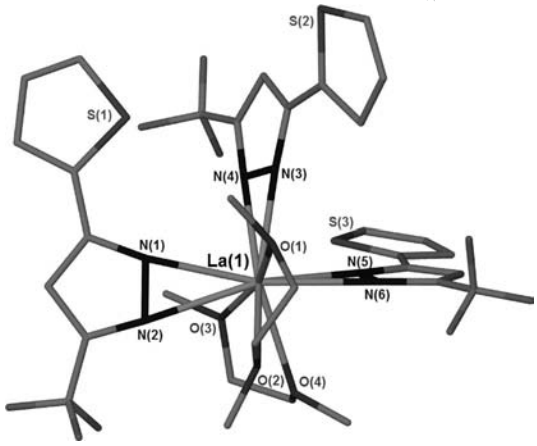

Figure 3. Crystal structure of **8a** (also representative of **8b** and **9**). All hydrogen atoms omitted for clarity.

The change from ten-coordination with two chelating dme ligands in **8a**, **8b** and **9** to nine-coordination in $[Ln(Ph_2pz)_3(dme)_2]$ (Ln = Nd,[19,28b] Eu,[19] Er[29]) with one unidentate and one chelating dme ligand, indicates that ttfpz is less bulky than Ph_2pz. Average Ln–N bond length differences in the nine-coordinate Ph_2pz complexes (0.018, 0.028 and 0.049 Å for RE = Nd, Eu and Er, respectively) are smaller than those of **8a**, **8b** and **9**, whereas in eight-coordinate $[Yb(Ph_2pz)_3(dme)]$,[16] two of three Ph_2pz ligands are substantially asymmetrically chelated.

Table 5. Crystallographic data for **8a**, **8b** and **9**.

	8a	**8b**	**9**
Chemical formula	$C_{32}H_{32}F_9LaN_6O_4S_3$	$2(C_{32}H_{32}F_9LaN_6O_4S_3)\cdot C_4H_{10}O$	$C_{32}H_{32}EuF_9N_6O_4S_3\cdot C_4H_{10}O_2$
Formula mass	970.73	2015.57	1073.90
Crystal system	monoclinic	monoclinic	monoclinic
Space group	*Cc*	$P2_1/n$	$P2_1/n$
a/Å	16.7332(4)	15.2098(2)	15.2611(4)
b/Å	14.7545(4)	40.7241(7)	41.3587(10)
c/Å	17.0284(4)	15.8987(3)	15.3792(4)
β/°	108.087(1)	115.984(1)	114.479(1)
Unit cell volume/Å^3	3996.40(17)	8852.3(3)	8834.5(4)
Number of formula units per unit cell, Z	4	4	8
Number of reflections measured	40901	94637	118184
Number of independent reflections	9059	20295	20247
R_{int}	0.0231	0.0507	0.0666
Final R_1 values [$I > 2\sigma(I)$]	0.0199	0.0887	0.0588
Final $wR(F^2)$ values [$I > 2\sigma(I)$]	0.0533	0.2223	0.1045
Final R_1 values (all data)	0.0210	0.1115	0.0910
Final $wR(F^2)$ values (all data)	0.0543	0.2378	0.1156
Goodness-of-fit on F^2	1.076	1.074	1.041

Table 6. Selected bond lengths [Å] and angles [°] for complexes **8a**, **8b** and **9**.

	8a	**8b**	**9**
Bond lengths			
RE(1)–N(1)	2.550(2)	2.566(7)	2.420(4)
RE(1)–N(2)	2.639(2)	2.615(7)	2.495(5)
RE(1)–N(3)	2.504(2)	2.470(7)	2.426(4)
RE(1)–N(4)	2.608(2)	2.604(7)	2.495(5)
RE(1)–N(5)	2.514(2)	2.515(7)	2.436(4)
RE(1)–N(6)	2.592(2)	2.586(7)	2.457(5)
RE(1)–O(1)	2.598(2)	2.691(6)	2.573(4)
RE(1)–O(2)	2.7040(18)	2.607(8)	2.617(4)
RE(1)–O(3)	2.5978(18)	2.578(6)	2.544(4)
RE(1)–O(4)	2.6794(19)	2.668(7)	2.555(4)
Centroid angles[a]			
cen{O(1)O(2)}–Ln–cen{O(3)O(4)}	122.12	126.32	123.25
cen{N(1)N(2)}–Ln–cen{N(3)N(4)}	96.08	101.72	99.36
cen{N(3)N(4)}–Ln–cen{N(5)N(6)}	83.51	83.83	82.46
cen{N(1)N(2)}–Ln–cen{N(5)N(6)}	173.76	172.17	178.18

[a] Centroid positions not refined.

In comparison with ten-coordinate **8a**, **8b** and **9** and nine-coordinate $[Eu(Ph_2pz)_3(dme)_2]$,[19] the eight-coordinate anion in the charge-separated $[Li(dme)_3][Eu^{II}(\eta^2\text{-}Ph_2pz)_3(dme)]$[30] complex appears to be a structural anomaly, since Eu^{2+} possesses a larger ionic radius than Eu^{3+}. Possibly, the lower charge on the metal together with the anionic nature of the complex leads to coordination saturation without steric saturation. With the tBu$_2$pz ligand, relevant structures are those of $[RE(t\text{Bu}_2pz)_3(\mu\text{-dme})]_n$ (RE = Nd,[29] Eu[31]) in which the metal is eight-coordinate with the single dme ligand exhibiting μ-*O*,*O*′ coordination. Together with the foregoing data, this indicates increasing steric bulk in the sequence ttfpz < Ph_2pz < tBu$_2$pz.

Conclusions

The complexes presented herein are the first examples of crystallographically characterised trivalent rare earth pyrazolate complexes bearing an unsymmetrically substituted pyrazolate ligand. For **1**–**3**, the structures change from a *fac*-arrangement in **1** and **2** to a *mer*-arrangement in **3**. By contrast, the related Ph_2pz complexes show the ligands arranged in a *mer*-fashion for $[Ln(Ph_2pz)_3(thf)_3]$ (Ln = Nd,[18] Sm).[19] In **4**–**7**, the coordination number is lowered to eight following the lanthanoid contraction. For the Ph_2pz analogues, only $[Yb(Ph_2pz)_3(thf)_2]$ has been crystallographically characterised but isolation of $[Gd(Ph_2pz)_3(thf)_2]$ suggests that the change to eight-coordination occurs for smaller Ln^{3+} for ttfpz. There is evidence from the RE–O bond lengths that ttfpz is less bulky than Ph_2pz. The dme-chelated ten-coordinate compounds **8a**, **8b** and **9** differ from $[RE(Ph_2pz)_3(dme)_2]$ complexes, which are nine-coordinate, and from $[RE(t\text{Bu}_2pz)_3(\mu\text{-dme})]_n$ complexes, which are eight-coordinate, and show that ttfpz has less steric bulk than Ph_2pz and tBu$_2$pz (Scheme 3). Thus, although η^2-coordination of the pyrazolate ligands is maintained with the unsymmetrical ttfpz ligand, there are significant differences from the coordination behaviour of the symmetrical Ph_2pz and tBu$_2$pz ligands, and these effects are more pronounced than for $[M(ttfpz)_2(solv)_n]$ (M = Ca, Sr, Ba, Yb).[13] Most of the complexes were prepared by redox transmetallation/protolysis from the metals, $Hg(C_6F_5)_2$ and ttfpzH, but **3** was obtained in low yield from the direct reaction of iodine-activated Tb metal with the pyrazole ligand.

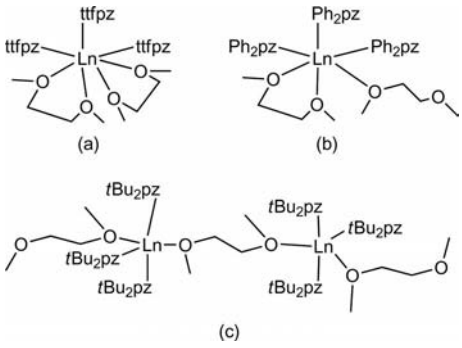

Scheme 3. Comparison of (a) 10-coordinate $[Ln(\eta^2\text{-ttfpz})_3(\eta^2\text{-dme})_2]$, (b) nine-coordinate $[Ln(\eta^2\text{-}Ph_2pz)_3(\kappa^1\text{-dme})(\kappa^2\text{-dme})]$ and (c) eight-coordinate $[Ln(\eta^2\text{-}t\text{Bu}_2pz)_3(\mu\text{-dme})]_n$.

Experimental Section

General Remarks: All reactions were carried out under dry nitrogen using standard Schlenk and dry box equipment; thf, Et_2O and dme were freshly distilled over sodium/benzophenone, and toluene from Na. Infrared spectra (4000–600 cm^{-1}) were recorded as Nujol mulls with a Perkin–Elmer Spectrum RX1 spectrometer. ^{1}H and ^{19}F NMR measurements were performed with a Bruker DPX 300 MHz spectrometer using dry, degassed deuterated benzene as solvent. The metal analysis of **9** was performed by EDTA titration with Xylenol Orange indicator and hexamine buffer after digestion with hydrochloric acid. Microanalysis samples were sealed in glass ampoules under purified N_2 and were determined by the Campbell Microanalytical service, University of Otago, New Zealand. 3-(2′-Thienyl)-5-(trifluoromethyl)pyrazole[32] and bis(pentafluorophenyl)mercury[33] were prepared according to literature methods.

General Procedure: Metal filings, ttfpzH and $Hg(C_6F_5)_2$ were stirred in the corresponding solvent for 2–4 days at ambient temperature. The resulting suspensions were filtered and single crystals were obtained from the concentrated solutions.

$[La(ttfpz)_3(thf)_3]\cdot 0.5PhMe$ (1): La metal (0.60 g, 4.30 mmol), ttfpzH (0.50 g, 2.30 mmol) and $Hg(C_6F_5)_2$ (0.60 g, 1.15 mmol) in thf (30 mL) for 2 days gave colourless crystals after removal of thf and recrystallisation from PhMe; yield 0.38 g, 47%; m.p. 130 °C. IR (Nujol mull): $\tilde{\nu}$ = 1794 (w), 1560 (w), 1354 (s), 1310 (m), 1245 (s), 1208 (s), 1171 (s), 1117 (m, br), 1079 (m), 981 (s), 925 (m), 846 (m), 805 (w), 790 (m), 727 (s), 693 (m) cm^{-1}. ^{1}H NMR (300 MHz, C_6D_6): δ = 7.37–7.35 (m, 3 H), 7.24 (s, 3 H), 6.91–6.86 (m, 6 H), 3.52 [m, 12 H, α-CH_2 (thf)], 2.19 [s, 1 H, CH_3 (PhMe)], 1.09 [m, 12 H, β-CH_2 (thf)] ppm; toluene peaks for the aromatic region were overshadowed by the solvent resonances. ^{19}F NMR (282 MHz, C_6D_6): δ = –60.02 ppm. $C_{39.5}H_{40}F_9LaN_6O_3S_3$ (1052.87): calcd. C 45.06, H 3.82, N 7.98; found C 44.91, H 3.71, N 8.12.

$[Sm(ttfpz)_3(thf)_3]$ (2): Sm metal (0.50 g, 3.32 mmol), ttfpzH (0.50 g, 2.30 mmol) and $Hg(C_6F_5)_2$ (0.60 g, 1.15 mmol) in thf (30 mL) for 3 d gave colourless crystals after removal of thf in vacuo and

recrystallisation from Et_2O; yield 0.36 g, 46%; m.p. 120 °C. IR (Nujol mull): $\tilde{\nu}$ = 1794 (w), 1578 (w), 1354 (m), 1312 (m), 1246 (s), 1208 (s), 1175 (s), 1117 (m, br), 1082 (m), 982 (s), 926 (m), 849 (m), 808 (m), 789 (m), 691 (m) cm^{-1}. ^1H NMR (300 MHz, C_6D_6): δ = 7.98 (m, 3 H), 7.22 (m, 3 H), 6.99–6.93 (m, 6 H), 1.39 [s, 12 H, α-CH_2 (thf)], 0.13 [s, 12 H, β-CH_2 (thf)] ppm. ^{19}F NMR (282 MHz, C_6D_6): δ = –59.37 ppm. $C_{36}H_{36}F_9N_6O_3S_3Sm$ (1018.25): calcd. C 42.46, H 3.56, N 8.25; found C 42.44, H 3.70, N 8.46.

[Tb(ttfpz)$_3$(thf)$_3$]·thf (3): Tb metal filings (0.60 g, 3.77 mmol), ttfpzH (0.40 g, 1.83 mmol) and a few small crystals of iodine (≈ 0.3 mmol) were stirred in thf for 3 d at ambient temperature. The suspension was filtered through a filter cannula and the pale yellow coloured filtrate was concentrated in vacuo. Yellow crystals were obtained from the concentrated solution after one week at –20 °C; yield 0.11 g, 17%; m.p. 122 °C. IR (as Nujol mull): $\tilde{\nu}$ = 1799 (w), 1561 (m), 1353 (s), 1312 (s), 1247 (vs), 1209 (vs), 1170 (s), 1128 (vs, br), 1078 (vs), 985 (vs), 926 (s), 846 (vs), 805 (s), 720 (s), 694 (vs) cm^{-1}. No satisfactory ^1H NMR spectrum owing to paramagnetism. $C_{40}H_{44}F_9N_6O_4S_3Tb$ (1098.92): calcd. C 43.71, H 4.03, N 7.64; found C 41.27, H 3.44, N 8.10. For loss of lattice thf: calcd. for $C_{36}H_{36}F_9N_6O_3S_3Tb$ (1026.82): C, 42.10; H, 3.53; N, 8.18.

[Y(ttfpz)$_3$(thf)$_2$] (4): Y metal (0.50 g, 5.62 mmol), ttfpzH (0.40 g, 1.83 mmol) and $Hg(C_6F_5)_2$ (0.60 g, 1.15 mmol) in thf (30 mL) for 4 d gave yellow crystals after removal of thf in vacuo and recrystallisation from Et_2O; yield 0.35 g, 66%; m.p. (dec) 148 °C. IR (Nujol mull): $\tilde{\nu}$ = 1797 (w), 1560 (w), 1355 (m), 1312 (m), 1248 (s), 1210 (m), 1174 (s), 1127 (br)s, 1078 (m), 985 (s), 926 (m), 848 (m), 804 (m), 720 (m), 694 (m) cm^{-1}. ^1H NMR (300 MHz, C_6D_6): δ = 7.28–7.25 (m, 6 H), 6.86–6.79 (m, 6 H), 3.53 [s, 8 H, α-CH_2 (thf)], 1.02 [s, 8 H, β-CH_2 (thf)] ppm. ^{19}F NMR (282 MHz, C_6D_6): δ = –60.53 ppm. $C_{32}H_{28}F_9N_6O_2S_3Y$ (884.69): calcd. C 43.44, H 3.19, N 9.49; found C 43.19, H 3.08, N 9.64.

[Ho(ttfpz)$_3$(thf)$_2$] (5): Ho metal (0.50 g, 5.11 mmol), ttfpzH (0.50 g, 2.30 mmol) and $Hg(C_6F_5)_2$ (0.60 g, 1.15 mmol) in thf (30 mL) for 2 d gave pink crystals after removal of thf in vacuo and recrystallisation from Et_2O; yield 0.42 g, 58%; m.p. 108–112 °C. IR (Nujol mull): $\tilde{\nu}$ = 1798 (w), 1560 (w), 1355 (m), 1310 (m), 1248 (m), 1210 (m), 1128 (vs, br), 1078 (m), 984 (m), 925 (m), 848 (m), 803 (m), 721 (m), 702 (m) cm^{-1}. No satisfactory ^1H NMR spectrum owing to paramagnetism. $C_{32}H_{28}F_9HoN_6O_2S_3$ (960.71): calcd. C 40.00, H 2.93, N 8.74; found C 39.40, H 2.99, N 9.30.

[Lu(ttfpz)$_3$(thf)$_2$] (6): Lu metal (0.50 g, 2.85 mmol), ttfpzH (0.40 g, 1.83 mmol) and $Hg(C_6F_5)_2$ (0.47 g, 0.91 mmol) in thf (30 mL) for 4 d gave yellow crystals after removal of thf in vacuo and recrystallisation from Et_2O; yield 0.46 g, 79%; m.p. 140–144 °C. IR (Nujol mull): $\tilde{\nu}$ = 1798 (w), 1561 (m), 1355 (m), 1313 (m), 1248 (s), 1210 (s), 1175 (s), 1127 (vs, br), 1078 (m), 987 (s), 927 (m), 848 (s), 812 (m), 720 (m), 695 (s) cm^{-1}. ^1H NMR (300 MHz, C_6D_6): δ = 7.12–7.09 (m, 6 H), 6.73–6.67 (m, 6 H), 3.43 [s, 8 H, α-CH_2 (thf)], 0.91 [s, 8 H, β-CH_2 (thf)] ppm. ^{19}F NMR (282 MHz, C_6D_6): δ = –60.50 ppm. $C_{32}H_{28}F_9LuN_6O_2S_3$ (970.75): calcd. C 39.58, H 2.90, N 8.66; found C 39.38, H 3.09, N 8.64.

[Sc(ttfpz)$_3$(thf)$_2$] (7): Sc metal (0.30 g, 6.67 mmol), ttfpzH (0.40 g, 1.83 mmol) and $Hg(C_6F_5)_2$ (0.49 g, 0.915 mmol) in thf (30 mL) for 2 d gave colourless crystals from a concentrated solution within 7 d at ambient temperature; yield 0.37 g, 72%; m.p. 111 °C. IR (Nujol mull): $\tilde{\nu}$ = 1798 (w), 1600 (w), 1354 (s), 1311 (m), 1248 (s), 1211 (m), 1142 (m, br), 1079 (m), 984 (m), 927 (m), 848 (m), 803 (m), 720 (s), 699 (m) cm^{-1}. ^1H NMR (300 MHz, C_6D_6): δ = 6.98 (m, 6 H), 6.71–6.66 (m, 6 H), 3.49 [br., 8 H, α-CH_2 (thf)], 0.97 [br., 8 H, β-CH_2 (thf)] ppm. ^{19}F NMR (282 MHz, C_6D_6): δ = –60.58 ppm. $C_{32}H_{28}F_9N_6O_2S_3Sc$ (840.74): calcd. C 45.71, H 3.35, N 9.99; found C 44.88, H 3.25, N 10.24.

[La(ttfpz)$_3$(dme)$_2$] (8a) and [La(ttfpz)$_3$(dme)$_2$]·0.5Et$_2$O (8b): La metal (0.50 g, 3.60 mmol), ttfpzH (0.40 g, 1.83 mmol) and $Hg(C_6F_5)_2$ (0.48 g, 0.91 mmol) in dme (30 mL) for 3 d gave colourless crystals of **8a** directly from a concentrated dme solution, removal thereof and recrystallisation of a small sample from Et_2O gave **8b**. For **8a**: yield 0.45 g, 76%; dec. temp.: 130 °C. IR (Nujol mull): $\tilde{\nu}$ = 1797 (w), 1605 (w), 1558 (w), 1523 (s), 1308 (s), 1244 (s), 1212 (s), 1116 (s, br), 1051 (s), 987 (s), 924 (m), 842 (s), 734 (m), 640 (w) cm^{-1}. ^1H NMR (300 MHz, C_6D_6): δ = 7.35 (s, 3 H), 7.31 (m, 3 H), 6.98 (m, 6 H), 3.17 [s, 8 H, CH_2 (dme)], 3.04 [s, 12 H, CH_3 (dme)] ppm. ^{19}F NMR (282 MHz, C_6D_6): δ = –59.21 ppm. $C_{32}H_{32}F_9LaN_6O_4S_3$ (970.72) (**8a**): calcd. C 39.59, H 3.32, N 8.65; found C 39.54, H 3.45, N 8.41.

[Eu(ttfpz)$_3$(dme)$_2$]·dme (9): Eu metal (0.50 g, 3.30 mmol), ttfpzH (0.40 g, 1.83 mmol) and $Hg(C_6F_5)_2$ (0.47 g, 0.91 mmol) in dme (30 mL) for 4 d gave orange crystals from the gel-like concentrated dme solution after 6 months at –20 °C; yield 0.28 g, 43%; m.p. 105 °C. IR (as Nujol mull): $\tilde{\nu}$ = 1800 (w), 1606 (w), 1558 (w), 1517 (s), 1309 (s), 1246 (s), 1210 (s), 1114 (s, br), 1050 (s), 985 (s), 924 (m), 842 (s), 739 (m), 644 (w) cm^{-1}. No satisfactory ^1H NMR spectrum owing to paramagnetism. $C_{36}H_{42}EuF_9N_6O_6S_3$ (1073.89): calcd. Eu 15.44; found Eu 17.52. Calcd. for $C_{28}H_{22}EuF_9N_6O_4S_3$ (loss of two dme molecules): Eu 17.00%.

Blank reactions between Y, Eu or Tb metals and ttfpzH were carried out in a comparable manner to the above syntheses in thf for 5 d at room temperature. Workup gave crystalline ttfpzH (unit cell identification).

Attempted reaction between ttfpzH and $Hg(C_6F_5)_2$ on a 2:1 mol ratio in thf for 2 d gave only reactants (^1H and ^{19}F NMR identification).

Crystallography: Low-temperature single-crystal X-ray diffraction experiments were performed with a Bruker Apex II CCD with Mo-K_α radiation (λ = 0.71073 Å) and equipped with an Oxford Instruments nitrogen gas cryostream. Single crystals were mounted on a glass fibre in viscous hydrocarbon oil and quench-cooled to 123(2) K. Analysis of diffraction data collected with the Bruker Apex II CCD was performed with SAINT+ within the APEX2[34] software package. Empirical absorption corrections were applied to all data using SADABS.[35] The structures were solved using SHELXS[36] and refined using SHELXL-97[36] within the graphical interface X-SEED.[37]

CCDC-816449 (for **1**), -816450 (for **2**), -816451 (for **3**), -816452 (for **4**), -816453 (for **5**), -816454 (for **6**), -816455 (for **7**), -816456 (for **8a**), -816457 (for **8b**) and -816458 (for **9**) contain the supplementary crystallographic data for this paper. These data (excluding structure factors) can be obtained free of charge from The Cambridge Crystallographic Data Centre via www.ccdc.cam.ac.uk/data_request/cif.

Crystallographic Disorder in 1–9: The disordered crystal structures (up to 20% of the atoms in the crystal structures are part of disorder) were modelled following this general approach: the 2-thienyl groups were disordered over two positions and their occupancies were freely refined against each other. DFIX, DANG and in some cases also FLAT, SIMU and/or ISOR restraints as well as the EADP constraint were applied on some/all atoms of the disordered components. Similarly, the fluorine atoms of CF_3 groups, where disorder was modelled, were restrained with DFIX and DANG, and sometimes SIMU and/or ISOR as well as EADP. Where applicable, the disordered coordinated solvent molecules were also modelled. **1**: Refined occupancies for thienyl groups S(1), S(2) and S(3)

were 75:25, 51:49 and 79:21, respectively. **2**: Refined occupancies for thienyl groups S(1), S(2) and S(3) were 86:14, 68:32 and 67:33, respectively. **3**: The rotational disorder of thienyl groups was small and therefore not modelled. The terminal CF_3 group on C(16) was modelled as described in the general approach, but occupancies were set at 80:20, and some fluorine atoms were additionally restrained using ISOR. Additionally, disordered thf molecules O(4/5) (occupancies set at 55:45) were restrained using DFIX, DANG and ISOR. **4**: the rotational disorder of thienyl groups was small and therefore not modelled. The terminal CF_3 group were modelled as described in the general approach, and occupancies were freely refined to be 53:37 [C(8)], 35:65 [C(16)] and 62:38 [C(24)]. Fluorine atoms were additionally restrained using ISOR. **5**: The rotational disorder of thienyl groups was small and therefore not modelled. The terminal CF_3 group on C(16) was modelled as described in the general approach, and occupancies were freely refined to be 75:25. Fluorine atoms were additionally restrained using ISOR. **6**: Refined occupancy for disordered thienyl group S(1) was 83:17. Refined occupancy for disordered CF_3 group on C(16) was 69:31. **7**: Refined occupancies for thienyl groups S(1) and S(3) were 77:23 and 73:27, respectively. **8a**: Attempts to solve the structure in *C*2/*c* were unsuccessful. Refined occupancy (*Cc* solution) for the disordered thienyl group S(3) was 52:48. Refined occupancies for disordered CF_3 group on C(16) and C(24) were 80:20 and 48:52, respectively. A search using PLATON found no higher symmetry in space group *Cc*. **8b**: Refined occupancies for thienyl groups S(1) and S(3–6) were 69:31, 71:29, 48:52, 64:36 and 71:29, respectively. **9**: Refined occupancies for thienyl groups S(1–6) were 61:39, 80:20, 47:53, 79:21, 63:37 and 54:56, respectively.

Acknowledgments

We are grateful to the Australian Research Council (grant DP0984775), the Faculty of Science for support and to Monash University for a Postgraduate Publications Award to A. U.

[1] M. A. Halcrow, *Dalton Trans.* **2009**, 2059–2073.
[2] J. E. Cosgriff, G. B. Deacon, *Angew. Chem.* **1998**, *110*, 298; *Angew. Chem. Int. Ed.* **1998**, *37*, 286–287.
[3] C. L. Dezelah, M. K. Wiedmann, K. Mizohata, R. J. Baird, L. Niinisto, C. H. Winter, *J. Am. Chem. Soc.* **2007**, *129*, 12370–12371.
[4] O. M. El-Kadri, M. J. Heeg, C. H. Winter, *J. Organomet. Chem.* **2009**, *694*, 3902–3911.
[5] J. G. Cederberg, T. D. Culp, B. Bieg, D. Pfeiffer, C. H. Winter, K. L. Bray, T. F. Kuech, *J. Cryst. Growth* **1998**, *195*, 105–111.
[6] T. D. Culp, J. G. Cederberg, B. Bieg, T. F. Kuech, K. L. Bray, D. Pfeiffer, C. H. Winter, *J. Appl. Phys.* **1998**, *83*, 4918–4927.
[7] J. G. Cederberg, T. D. Culp, B. Bieg, D. Pfeiffer, C. H. Winter, K. L. Bray, T. F. Kuech, *J. Appl. Phys.* **1999**, *85*, 1825–1831.
[8] J. Paivasaari, J. Niinisto, P. Myllymaki, C. Dezelah, C. H. Winter, M. Putkonen, M. Nieminen, L. Niinisto, *Topics Appl. Phys.* **2007**, *106*, 15–32.
[9] G. Meyer, *Z. Anorg. Allg. Chem.* **2008**, *634*, 201–222.
[10] G. B. Deacon, E. E. Delbridge, B. W. Skelton, A. H. White, *Eur. J. Inorg. Chem.* **1999**, 751–761.
[11] A. Y. O'Brien, J. Hitzbleck, A. Torvisco, G. B. Deacon, K. Ruhlandt-Senge, *Eur. J. Inorg. Chem.* **2008**, 172–182.
[12] Previously unused according to CCDC v5.31 and subsequent updates to 08/2010.
[13] G. B. Deacon, P. C. Junk, A. Urbatsch, *Dalton Trans.* **2011**, *40*, 1601–1609.
[14] J. Hitzbleck, A. Y. O'Brien, C. M. Forsyth, G. B. Deacon, K. Ruhlandt-Senge, *Chem. Eur. J.* **2004**, *10*, 3315–3323.
[15] R. D. Shannon, *Acta Crystallogr., Sect. A* **1976**, *32*, 751–767.
[16] S. Beaini, G. B. Deacon, E. E. Delbridge, P. C. Junk, B. W. Skelton, A. H. White, *Eur. J. Inorg. Chem.* **2008**, 4586–4596.
[17] S. Hamidi, G. B. Deacon, P. C. Junk, unpublished results, **2010**.
[18] J. E. Cosgriff, G. B. Deacon, B. M. Gatehouse, *Aust. J. Chem.* **1993**, *46*, 1881–1896.
[19] S. Beaini, G. B. Deacon, M. Hilder, P. C. Junk, D. R. Turner, *Eur. J. Inorg. Chem.* **2006**, 3434–3441.
[20] T. K. Panda, A. G. Trambitas, T. Bannenberg, C. G. Hrib, S. Randoll, P. G. Jones, M. Tamm, *Inorg. Chem.* **2009**, *48*, 5462–5472.
[21] G. B. Deacon, T. C. Feng, B. W. Skelton, A. H. White, *Aust. J. Chem.* **1995**, *48*, 741–756.
[22] D. Freedman, J. H. Melman, T. J. Emge, J. G. Brennan, *Inorg. Chem.* **1998**, *37*, 4162–4163.
[23] G. W. Rabe, C. S. Strissel, L. M. Liable-Sands, T. E. Concolino, A. L. Rheingold, *Inorg. Chem.* **1999**, *38*, 3446–3447.
[24] L. Clark, G. B. Deacon, C. M. Forsyth, P. C. Junk, P. Mountford, J. P. Townley, *Dalton Trans.* **2010**, *39*, 6693–6704.
[25] J. E. Cosgriff, G. B. Deacon, B. M. Gatehouse, H. Hemling, H. Schumann, *Angew. Chem.* **1993**, *105*, 906; *Angew. Chem. Int. Ed. Engl.* **1993**, *32*, 874–875.
[26] J. E. Cosgriff, G. B. Deacon, B. M. Gatehouse, H. Hemling, H. Schumann, *Aust. J. Chem.* **1994**, *47*, 1223–1235.
[27] G. B. Deacon, C. M. Forsyth, A. Gitlits, B. W. Skelton, A. H. White, *Dalton Trans.* **2004**, 1239–1247.
[28] a) J. E. Cosgriff, G. B. Deacon, B. M. Gatehouse, P. R. Leeb, H. Schumann, *Z. Anorg. Allg. Chem.* **1996**, *622*, 1399–1403; b) G. B. Deacon, E. E. Delbridge, G. D. Fallon, C. Jones, D. E. Hibbs, M. B. Hursthouse, B. W. Skelton, A. H. White, *Organometallics* **2000**, *19*, 1713–1721.
[29] J. E. Cosgriff, G. B. Deacon, G. D. Fallon, B. M. Gatehouse, H. Schumann, R. Weimann, *Chem. Ber.* **1996**, *129*, 953–958.
[30] S. Beaini, G. B. Deacon, C. M. Forsyth, P. C. Junk, *Z. Anorg. Allg. Chem.* **2008**, *634*, 2903–2906.
[31] E. E. Delbridge, Doctoral Thesis, Monash University, **1999**.
[32] K. A. Volkova, A. N. Volkov, A. I. Albanov, A. S. Nakhmanovich, V. A. Lopyrev, *Russ. J. Gen. Chem.* **2003**, *73*, 1623–1626.
[33] G. B. Deacon, J. E. Cosgriff, E. T. Lawrenz, C. M. Forsyth, D. L. Wilkinson, *Hermann-Brauer Synthetic Methods of Organometallic and Inorganic Chemistry* (Ed.: W. A. Herrmann), vol. 6 (Ed.: F. T. Edelmann), Thieme, Stuttgart, Germany, **1997**.
[34] Bruker AXS Ltd., Madison, WI, **2005**.
[35] G. M. Sheldrick, University of Göttingen, Germany, **1996**.
[36] G. M. Sheldrick, *Acta Crystallogr., Sect. A* **2008**, *64*, 112–122.
[37] L. J. Barbour, *J. Supramol. Chem.* **2001**, *1*, 189–191.

Received: May 12, 2011
Published Online: July 19, 2011

